crystals

MDPI

Article

Experimental Study of the Thermophysical Properties of the Red Earth Composite Stabilized with Cement Containing Waste Glass Powder

Oumaima Nasry [1,*], Abderrahim Samaouali [1,*], Hanane Sghiouri El Idrissi [1], Nora Bouhaddour [1] and Adil Hafidi Alaoui [2]

[1] Team Thermodynamic-Energy, Energy Research Center, Department of Physics, Faculty of Sciences, Mohammed V University, Rabat 10090, Morocco; hanane_sghiourielidrissi@um5.ac.ma (H.S.E.I.); nora_bouhaddour@um5.ac.ma (N.B.)

[2] Mechanical Laboratory and Civil Engineering, Faculty of Sciences and Technology, Abdelmalek Essaadi University, Tangier 93000, Morocco; pr_alaoui@yahoo.fr

* Correspondence: oumaima_nasry@um5.ac.ma (O.N.); abderrahimsamaouali@yahoo.fr (A.S.); Tel.: +212-6-02-84-09-56 (O.N.)

Abstract: The aim of this study was to measure the thermophysical properties (thermal conductivity, volumetric thermal capacity, thermal diffusivity, and thermal effusivity) of red earth stabilized with cement and substituted with waste glass powder. Several samples (red earth) were stabilized with 6% and 12% cement and incorporated with different percentages of waste glass powder, which varied from 10% to 30%. The bulk density of the 12 samples was measured in the dry state and at room temperature. All samples were analyzed by a scanning electron microscope (SEM). The thermal conductivity and specific heat of the composite materials were measured experimentally with a thermal conductivity device (CT meter) in the dry state and at ambient temperature. The experimental results showed a decrease in the thermophysical parameters of stabilized red earth containing 12% cement and substituted by 30% glass powder. The following results were obtained: 53.97% for thermal conductivity, 45.42% for volumetric specific heat, 15.66% for thermal diffusivity, and 49.88% for thermal effusivity. The bulk density of the red earth also decreased by 13.66% in the dry state at ambient temperature. Stabilization with 6% and 12% cement played an important role in the compactness of the material and, consequently, improved its thermophysical performance. The composition of this new ternary material significantly affected the thermophysical properties of the red earth.

Keywords: soda-lime waste glass; composite material; thermophysical properties; cement stabilized blocks; red earth

check for updates

Citation: Nasry, O.; Samaouali, A.; El Idrissi, H.S.; Bouhaddour, N.; Alaoui, A.H. Experimental Study of the Thermophysical Properties of the Red Earth Composite Stabilized with Cement Containing Waste Glass Powder. *Crystals* **2022**, *12*, 396. https://doi.org/10.3390/cryst12030396

Academic Editors: Nichola Coleman and Samantha E. Booth

Received: 31 January 2022
Accepted: 10 March 2022
Published: 15 March 2022

Publisher's Note: MDPI stays neutral with regard to jurisdictional claims in published maps and institutional affiliations.

Copyright: © 2022 by the authors. Licensee MDPI, Basel, Switzerland. This article is an open access article distributed under the terms and conditions of the Creative Commons Attribution (CC BY) license (https://creativecommons.org/licenses/by/4.0/).

1. Introduction

The acceleration of human activity for many years has had an impact on the natural environment. The energy consumption curve continues to increase. However, the reduction in flue gas, soot, and dust by energy conservation contributes directly to the protection of the environment. In the building sector, a solution is to increase the use of local materials and industrial waste in order to decrease the use of energy-intensive materials such as steel, concrete, and cement [1–5].

The use of locally sourced building materials has environmental and ecological benefits. Red earth in its natural state can be useful in many building materials without energy expenditure compared to concrete, steel, or cement [6]. Some properties of earth bricks (low density, low thermal conductivity) justify their use for improving thermal insulation [7–9]. The red earth from the local region of Rabat-Sale is the subject of this work.

The recycling of glass waste in construction materials has also been developed by several researchers [10–15]. The chemical composition of glass plays a very important role

in the development of the pozzolanic reaction and the reduction in the rate of alkali–silica reactions, which subsequently influences the physical and mechanical properties of materials based on waste glass [16]. A high content of glass modifiers (K, Na, Pb), in addition to a low amount of glass formers and stabilizers, favors the ASR reaction [16]. In this study, the ASR reaction was controlled only by choosing a type of glass with a high content of glass formers compared to glass modifiers, as well as by a substitution of glass powder limited to 30%. The ASR rate was proven to be faster with K than with Na [17]. The chemical composition of soda-lime glass satisfies the requirements to be used as a supplementary cementitious material due to its high content of glass formers and low content of glass modifiers.

In the literature, the manufacture of cement-stabilized compressed clay-based red earth blocks is beginning to emerge in research [18–20]. However, few studies are focused on the incorporation of glass powder in this composite material. The method of mixing and stabilization is one of the techniques studied for the production of building materials based on clay [21]. The mixing and stabilization method is based on the partial replacement of red earth with some wastes or byproducts and the addition of cementing materials such as cement. The purpose of this work was to study the thermal performance of cement-stabilized clay blocks as a function of the addition of glass powder. The water content of clay blocks mainly influences its density and thermal conductivity. The stabilization of clay blocks by cement must take into account the fact that cement needs water to set and act as a stabilizer; it also improves the resistance to compression and the resistance of the brick angles to abrasion and impact. According to the literature, the minimum percentage of stabilizing cement is 3% to 4% of the weight of the red earth used; however, for constructions that must resist rainwater, the percentage of cement should be increased to 10% [22].

The objective of this work was to conduct an experimental study on the variation of the thermophysical properties (thermal conductivity, thermal diffusivity, and specific heat) of cement-stabilized blocks (from 0% to 12%). A study of the variation of these different parameters according to the substitution of glass powder (from 0% to 30%) was also carried out. Microscopic characterizations using X-ray diffraction and scanning electron microscopy were performed to interpret the experimental results.

2. Materials and Methods

2.1. Materials

The soda-lime glass bottles were collected from municipal landfills. They were washed, crushed manually, and finely ground using a Funnel P-1 V2A (Idar-Oberstein, Germany) mechanical grinder until the desired powder was obtained. The particle size distribution is shown in Figure 1. The glass powder was ground until the resulting powder could pass through a 1 mm sieve mesh.

The Portland cement used was CPJ- CEM II 32,5 (LAFARGE, Paris, France) according to EN 197-1 [1]. This type of cement is often suitable for reinforced concrete, as well as for massive structures that require a moderate elevation of temperature. The cement presents a particle size of 100 µm.

The red earth from the Rabat-Sale region was manually sieved and dried in an oven at 105 °C for 24 h. The particle size distribution of the red earth is also shown in Figure 1. All the materials were dried in an oven to reach a moisture content of 0% before the preparation of the samples.

Table 1 presents the chemical compositions of the different dry materials. The soda-lime glass powder contained a large atomic percentage of oxygen and silicon, as well as a small atomic percentage of glass modifiers (K, Na, Pb). The red earth sample contained an atomic percentage of silicon and aluminum, as well as a small atomic amount of titanium and magnesium. The cement was characterized by a strong dominance of calcium, since it is the main component of the limestone that represents 80% of the raw material in the manufacture of Portland cement. The cement also contained a low composition of silicon,

aluminum, and sodium. These results were confirmed by XRD analysis of the different materials. Figure 2a shows that the main constituent of the red earth is quartz. Muscovite is also a mineral of the silicate group. XRD analysis of the glass powder shown in Figure 2b confirms the amorphous structure of the material. No crystalline peaks are clear. The XRD data of Portland cement shown in Figure 2c clearly indicate the presence of mainly alites and secondly belites, as well as less intense peaks representing aluminate and ferrite.

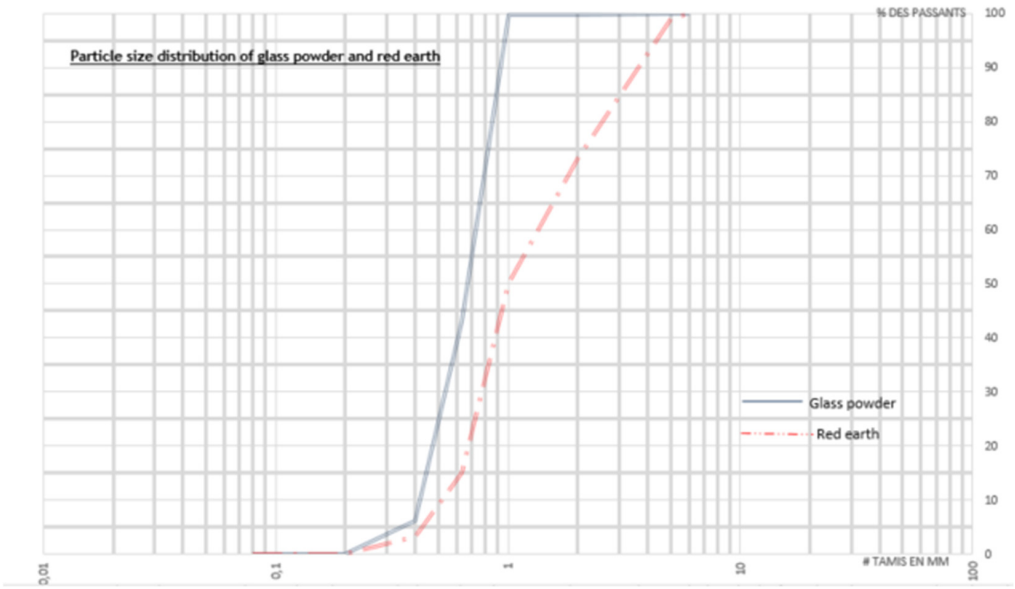


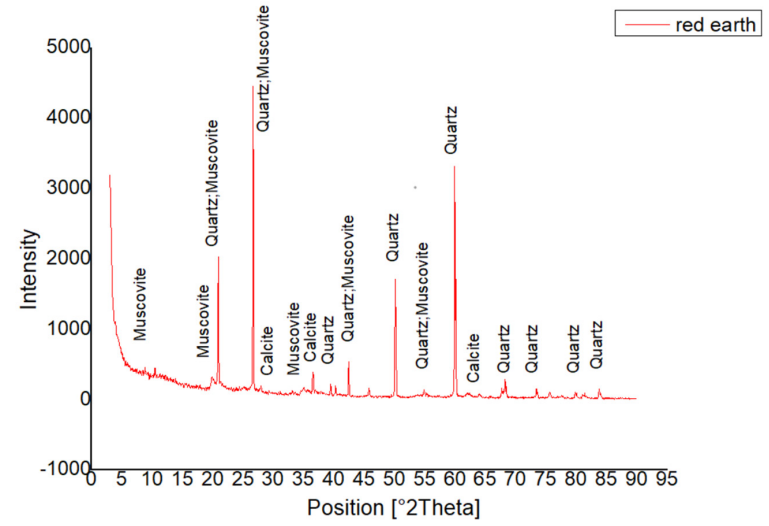
Figure 1. Particle size distribution of glass powder and red earth.

Table 1. Chemical composition of glass powder, cement and red earth.

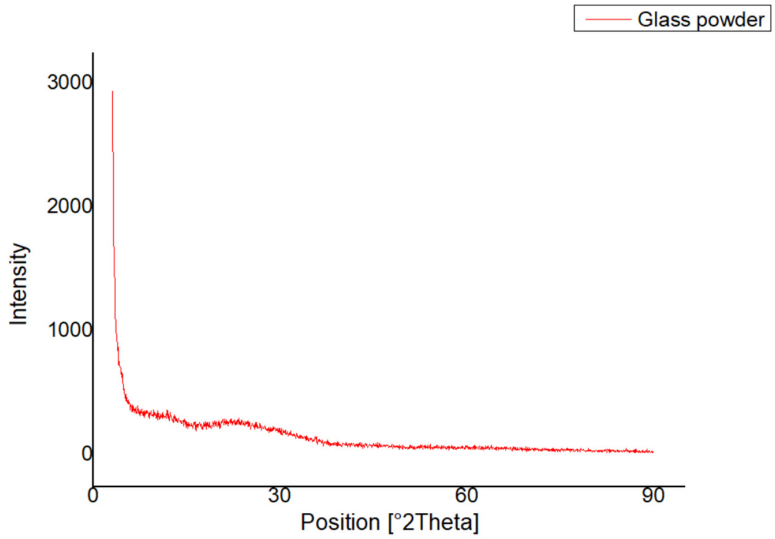
Element (at.%)	Glass Powder	Cement	Red Earth
O	42.77	44.49	48.62
Na	10.75	0.23	3.28
Mg	0.21	0.57	0.48
C	-	12.10	8.13
Al	0.8	1.92	11.15
Si	38.45	6.48	18.93
Ca	6.83	31.32	0.56
K	0.13	1.04	1.19
Ti	-	0.13	0.62
Fe	0.07	1.72	7.04
Total	100	100	100

2.2. Sample Preparation

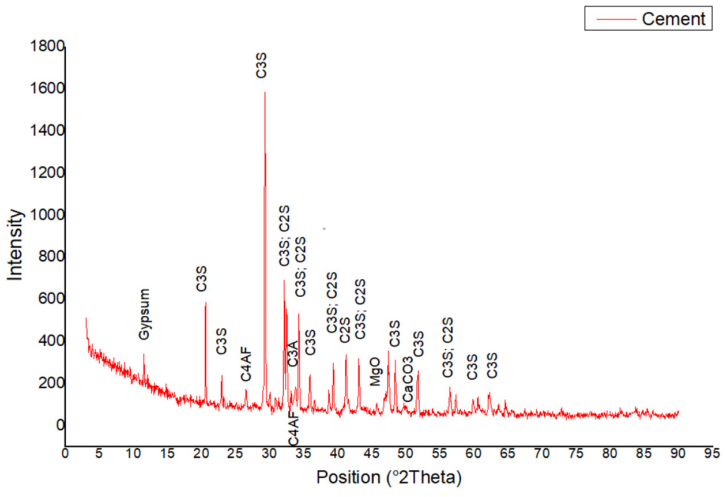
The control sample was composed of only red earth and water. Another set of samples was composed of red earth, cement, and glass powder. The glass powder was used as substitute of the red earth in percentages of 10%, 20%, and 30%. Red earth was replaced by 6% and 12% cement (Figure 3). The solid raw materials (cement, red earth, glass powder) were first mixed until homogenization, and then potable water was added. The water/binder ratio was 0.3 for all mixtures. After mixing, the samples were compacted on a vibrating table and then prepared in containers of 40 mm × 70 mm × 90 mm. The surface of the samples was covered with polyethylene to prevent moisture loss. All specimens were stored at 20 °C and RH 65%. The specimens were demolded after 48 h, and then cured under optimal conditions (20 °C and RH 65%) for 28 days. Table 2 summarizes the preparation of all samples. The thermal properties of the samples were measured in the dry state at 20 °C.



(**a**)



(**b**)



(**c**)

Figure 2. X-ray diffraction patterns of (**a**) red earth powder, (**b**) glass powder, and (**c**) cement.

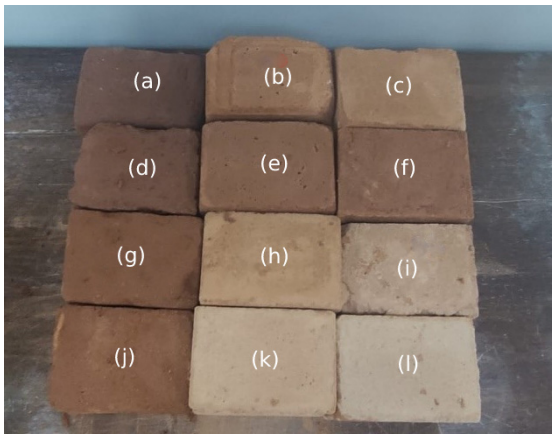


Figure 3. Samples of red earth blocks stabilized with cement and glass powder: (**a**) control sample (RSB); (**b**) 0% GP + 6% cement; (**c**) 0% GP + 12% cement; (**d**) 10% GP + 0% cement; (**e**) 10% GP + 6% cement; (**f**) 10% GP + 12% cement; (**g**) 20% GP + 0% cement; (**h**) 20% GP + 6% cement; (**i**) 20% GP + 12% cement; (**j**) 30% GP + 0% cement; (**k**) 30% GP + 6% cement; (**l**) 30% GP + 12% cement.

Table 2. Sampling of ternary composite materials.

	Code	Red Earth (g)	Water/Binder Ratio	Cement (g)	Glass Powder (g)
0% cement	Control sample (red earth brick (RSB))	1000	0.3	0	0
	RSB + 10%GP	900	0.3	0	100
	RSB + 20% GP	800	0.3	0	200
	RSB + 30%GP	700	0.3	0	300
6% cement	RSB 6	940	0.3	60	0
	RSB 6 + 10% GP	840	0.3	60	100
	RSB 6 + 20% GP	740	0.3	60	200
	RSB 6 + 30% GP	640	0.3	60	300
12% cement	RSB 12	900	0.3	120	0
	RSB 12 + 10% GP	780	0.3	120	100
	RSB 12 + 20% GP	680	0.3	120	200
	RSB 12 + 30% GP	580	0.3	120	300

2.3. Methods

X-ray powder diffraction patterns were collected at room temperature (25 °C), over the 2θ angle range of $10° \leq 2\theta \leq 60°$ with a step size of 0.04°, using a Siemens D5000 (Aubrey, Texas, USA) diffractometer operating in Bragg configuration with a copper anti-cathode with Kα = 1.54056 Å.

The morphology of the samples was verified using a scanning electron microscope JEOL IT 100 type MEOL (JEOL, Tokyo, Japan). In order to allow a minimum particle size of 4 nm, a thin layer of gold was useful to make the surface more conductive. The MEOL used in this study was associated with an energy-dispersive spectrometer (EDS) to determine the atomic composition of the sample.

The thermal properties were measured by a CT meter device (standard) delivered by the Modern Society of Electronic Studies (VOIRON, France). The flexible sonde in the form of a ring with a thickness of 0.2 mm (60 mm × 90 mm) and a radius of 10 mm was inserted between two similar samples. The heating resistance was 2.20 Ω, the power was 1 W, the heating time was 400 s, and the measurement time was 500 s. The sonde was connected to the device (CT meter) via a plug (Figure 4). Each measurement was the average of three measurements. The standard measurement uncertainty was 5%. The equipment used was developed by the CSTB (Technical and Scientific Center for Building). This type of sonde is

used to measure the thermal conductivity (W/m·K) and specific heat (kJ/m^3·K) of solid materials [23].

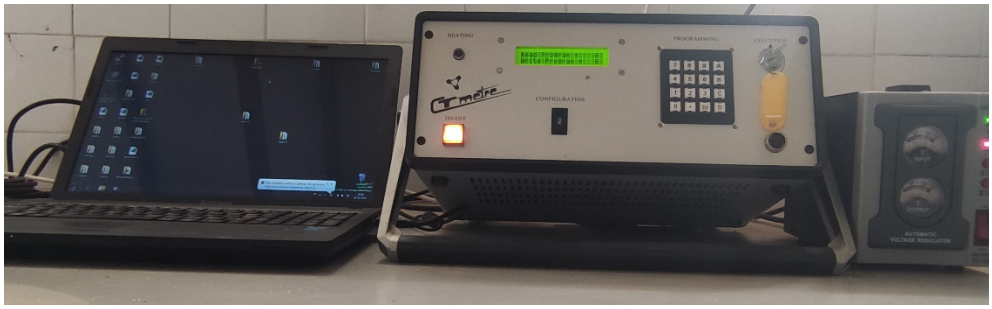
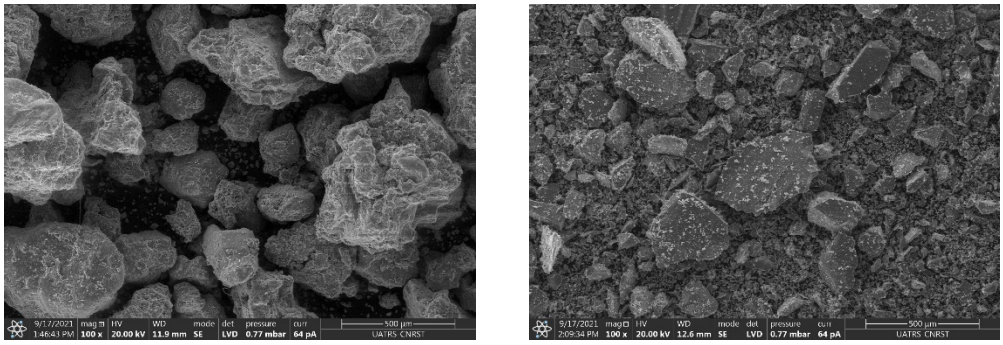


Figure 4. CT meter device.

3. Results and Discussions

3.1. X-ray Diffraction and Scanning Electron Microscopy (SEM)

The red earth powder and glass powder samples were characterized by scanning electron microscopy. The spherical morphology of the red earth is shown in Figure 5a. The texture and morphology of the glass powder were characterized by finer needle-shaped particles, as shown in Figure 5b.



(**a**) (**b**)

Figure 5. Scanning electron microscopy of (**a**) red earth powder, and (**b**) glass powder.

Figure 6 represents the microscopic characterization of the different samples of red earth bricks stabilized with 6% and 12% cement and substituted with 10% and 30% glass powder. The composite samples constituted by glass powder, cement, and red earth represent hydrated calcium silicates C–S–H formed as a reaction product of amorphous silica and portlandite. Amorphous silica in glass produces a Si-rich layer on the glass surface. This layer reacts with Ca^{2+} in the porous solution to form C–S–H. The morphology of the C–S–H gel produced by the hydration of cement appeared in a flocculent needle shape. It can be seen in Figure 6c,f that the red earth particles adhered to the surface of the glass powder; this bond strength between the red earth matrix and the glass powder was much higher due to the hydration products of cement that created a greater bond between the red earth particles and the glass powder. The agglomerations appeared as needles on the surface of the GP glass powder. The obtained results are in agreement with those of Jiang et al. [24].

The C–S–H grew on the surface of the unhydrated cement grains and gradually filled the capillary gaps between the grains. The presence of hydrates, composed of portlandite (CH) and hydrated calcium silicates (C–S–H), shows that red earth–cement bonds were formed, which enhanced the ability of the composite material to withstand mechanical stresses [20]. These hydrates, composed of portlandite (CH) platelets and hydrated calcium silicates (C–S–H) more or less compact, developed in the cement contact zone Figure 6c, as well as in the red earth matrix. This bond strengthening increased with cement content,

which explains why the samples were more compact with a higher cement content. The samples presented in Figure 6a,d,g do not show cement hydration. The porosity shown in Figure 6a could be due to the expansion of the clay elements presented in the red earth. The interfacial transition zone is presented mainly in Figure 6d. This could be due to the weak bonding of the red earth and glass powder matrix.

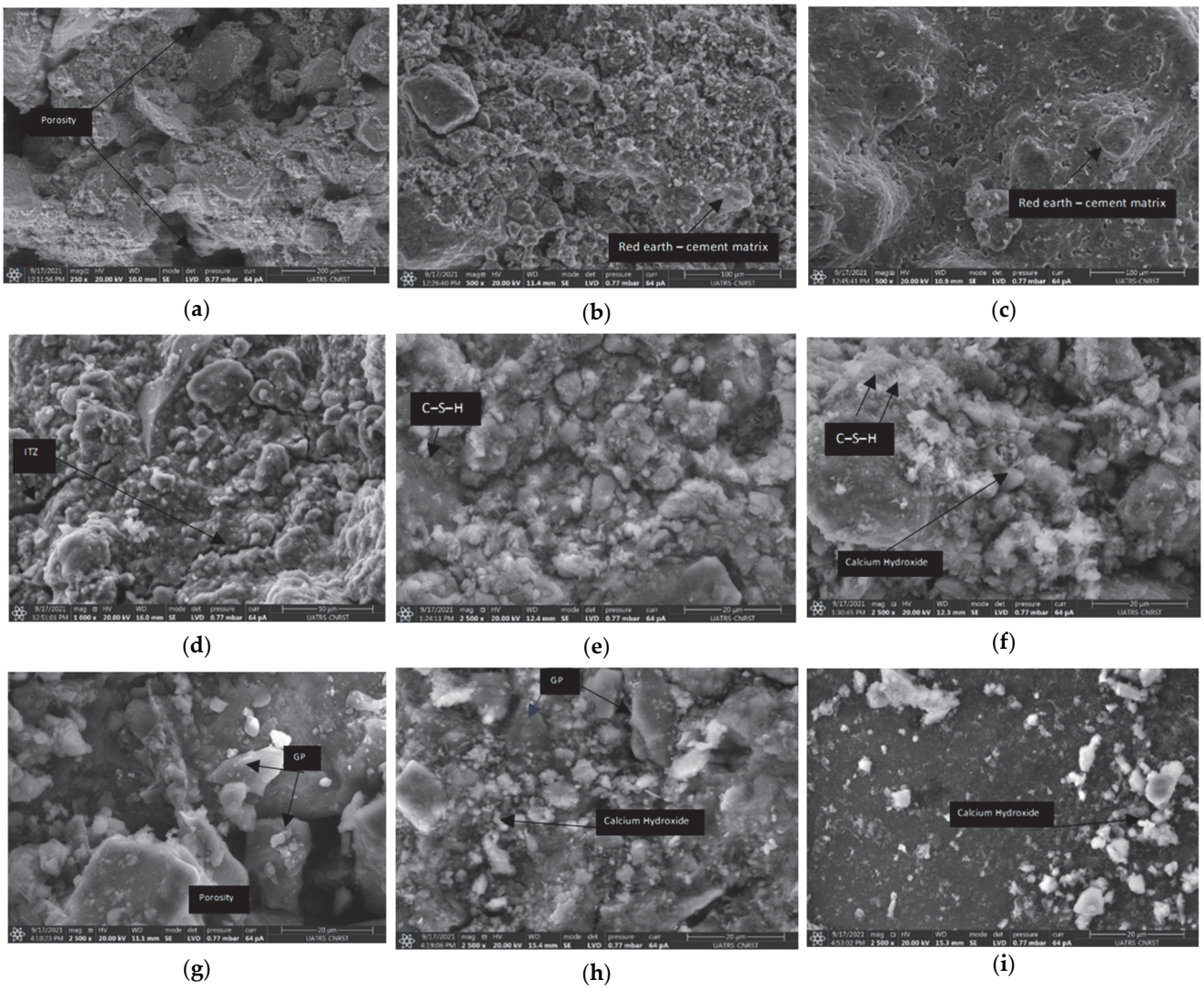


Figure 6. Scanning electron microscopy of ternary composite material sampling: (**a**) control sample (RSB); (**b**) 0% GP + 6% cement; (**c**) 0% GP + 12% cement; (**d**) 10% GP + 0% cement; (**e**) 10% GP + 6% cement; (**f**) 10% GP + 12% cement; (**g**) 30% GP + 0% cement; (**h**) 30% GP + 6% cement; (**i**) 30% GP + 12% cement.

Table 3 shows the qualitative chemical composition of the composite materials. The samples stabilized with cement and substituted with glass powder showed the presence of silicon and calcium, as well as an average atomic percentage of aluminum and iron. The sodium present in the glass powder, cement, and red earth could generate ASR reactions in the cement paste and, consequently, decrease the mechanical durability of the material.

The XRD analyses of the composite materials are presented in Figure 7. The samples were composed mainly of quartz minerals and calcite. This global analysis qualitatively indicated the dominant presence of quartz and calcite peaks.

Table 3. Chemical composition of (**a**) control sample (RSB), (**b**) 0% GP + 6% cement, (**c**) 0% GP + 12% cement, (**d**) 10% GP + 0% cement, (**e**) 10% GP + 6% cement, (**f**) 10% GP + 12% cement, (**g**) 30% GP + 0% cement, (**h**) 30% GP + 6% cement, and (**i**) 30% GP + 12% cement.

Element	a	b	c	d	e	f	g	h	i
C	4.35	5.29	7.26	4.19	4.40	5.83	7.47	7.58	8.68
O	52.83	53.18	54.94	50.21	52.58	51.85	52.28	52.80	52.28
Na	3.58	0.38	0.42	0.87	0.80	0.41	3.68	3.61	6.46
Mg	0.64	0.42	0.23	0.59	0.54	0.49	0.54	0.30	0.41
Al	4.91	8.23	4.82	9.01	9.22	9.10	4.36	4.20	2.32
Si	22.64	17.22	10.72	23.23	18.77	15.31	24.71	24.00	21.18
K	0.47	0.85	1.07	0.93	0.99	1.09	0.50	0.69	0.42
Ca	4.81	7.66	17.14	2.18	4.61	8.44	3.23	4.05	6.57
Ti	0.39	0.41	0.32	0.45	0.59	0.49	-	-	0.35
Fe	5.38	6.36	3.26	8.34	7.50	6.98	3.09	2.77	1.32
Total	100.00	100.00	100.00	100.00	100.00	100.00	100.00	100.00	100.00

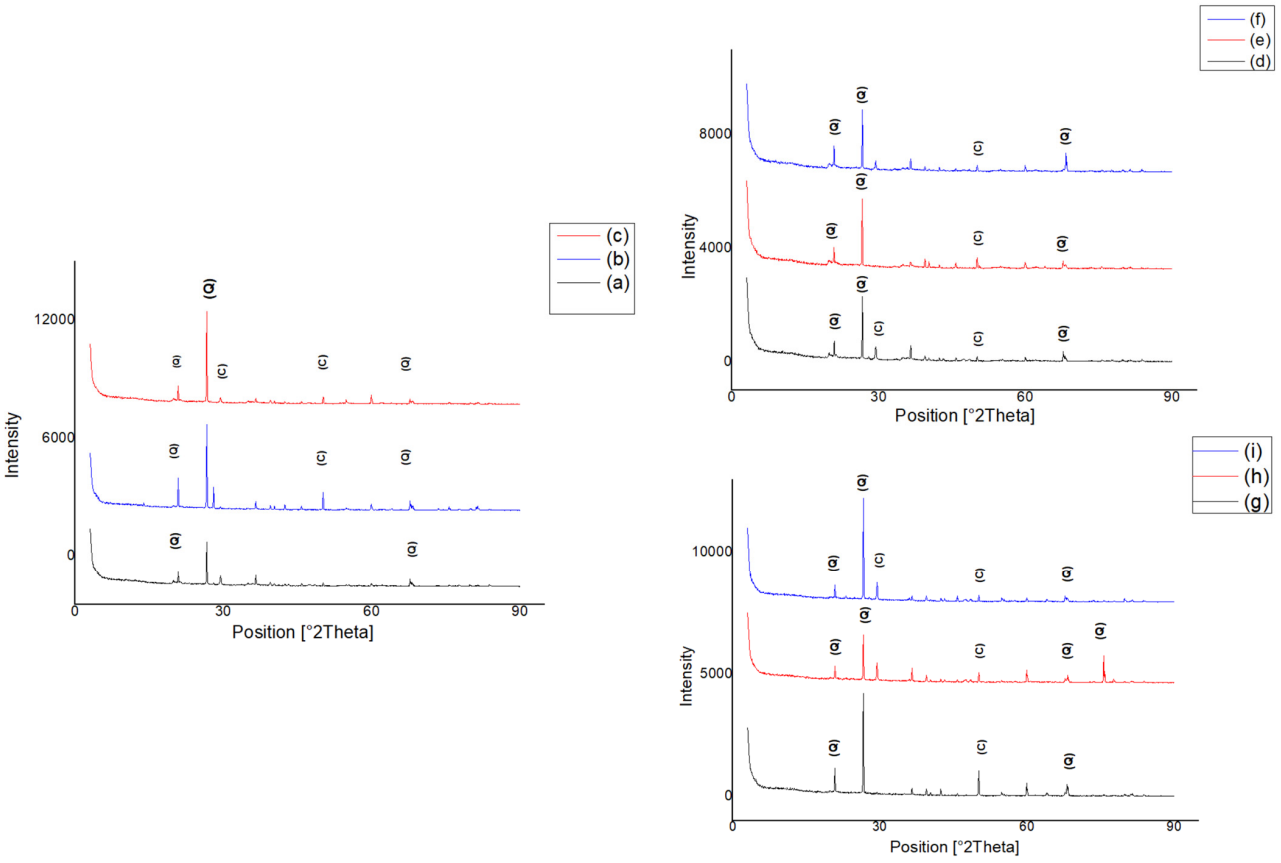


Figure 7. X-ray diffraction patterns: (**a**) control sample (RSB); (**b**) 0% GP + 6% cement; (**c**) 0% GP + 12% cement; (**d**) 10% GP + 0% cement; (**e**) 10% GP + 6% cement; (**f**) 10% GP + 12% cement (**g**) 30% GP + 0% cement; (**h**) 30% GP + 6% cement; (**i**) 30% GP + 12% cement. Q, quartz; C, calcite.

3.2. Thermo-Physical Properties

3.2.1. Relationship between Density and Thermal Conductivity

Figure 8 shows the densities of the glass powder-substituted and cement-stabilized red earth samples. The samples were measured in the dry state at ambient temperature. The density of the red earth blocks substituted with 0%, 10%, 20%, and 30% glass powder decreased slightly from 1.83 to 1.58 g/cm^3, a variation of 13.66%. Variations of 19.47% and 9.46% were also observed with the addition of 6% and 12% stabilizing cement, respectively

(Figure 6). The decrease in density with the addition of glass powder was mainly dependent on the increase in pore size of the sharp and pointed morphologies of the glass. The decrease in pore volume with the substitution of cement was due to the fineness of this material, which made the paste more compact. These results confirm the general laws of thermal conductivity for porous materials. This phenomenon for red earth blocks is similar to the studies of Zhang et al. [18] and Tang et al. [25].

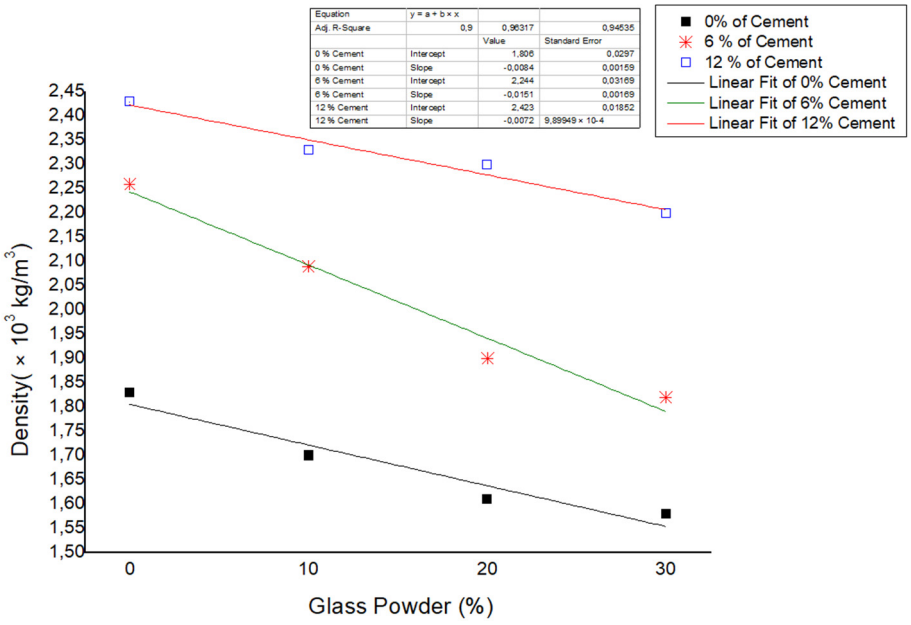


Figure 8. Variation of the measured bulk density in the dry state as a function of the glass powder content.

3.2.2. Effect of Glass Powder Content on Thermal Conductivity and Specific Heat Capacity

The thermal characterization of cement stabilized red earth samples substituted with glass powder was performed using a CT meter at a room temperature of 21 ± 1 °C (Figure 9). The thermal conductivity of the glass powder-substituted earth blocks decreased by 53.97% (from 1.334 W/m·K to 0.614 W/m·K), 47.22%, and 40.41% with the addition of 0%, 6%, and 12% cement, respectively. The decrease in thermal conductivity of red earth blocks substituted by glass powder was mainly due to the decrease in density and the subsequent increase in pore volume.

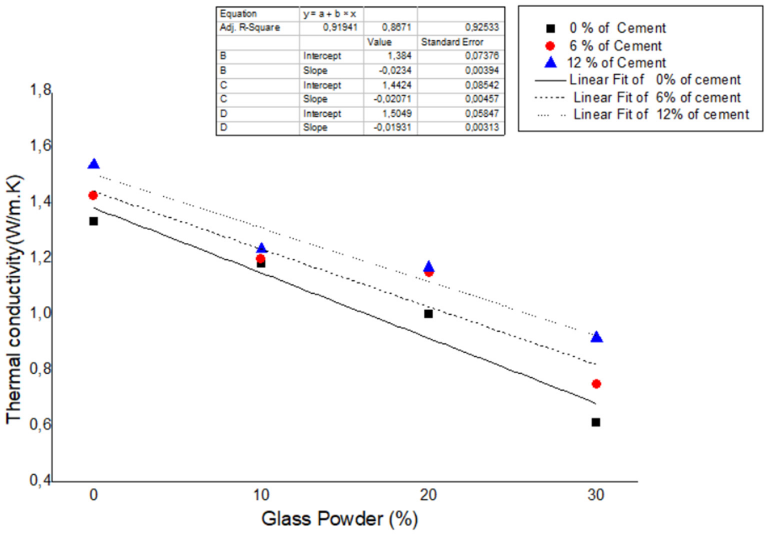


Figure 9. Variation of the measured mortars thermal conductivity in the dry state as a function of the glass powder content.

However, the thermal conductivity of red earth blocks increased with the addition of stabilizing cement. The spherical and fine morphology of the cement allowed for a decrease in porosity and, subsequently, a decrease in the pore volume of the materials. Tiskatine et al. also found that the cement particles increased the contact and bonding between the clay grains to ensure good compaction and, subsequently, an increase in the thermal conductivity of the material [26].

The specific heat capacity measurements of cement-stabilized red earth blocks as a function of glass powder substitution rate are shown in Figure 10. The specific heat of the glass powder-substituted samples decreased by 45.42%. A decrease was also recorded in the glass composite material with the addition of 6% and 12% cement, respectively, variations of 36.90% and 25.23%.

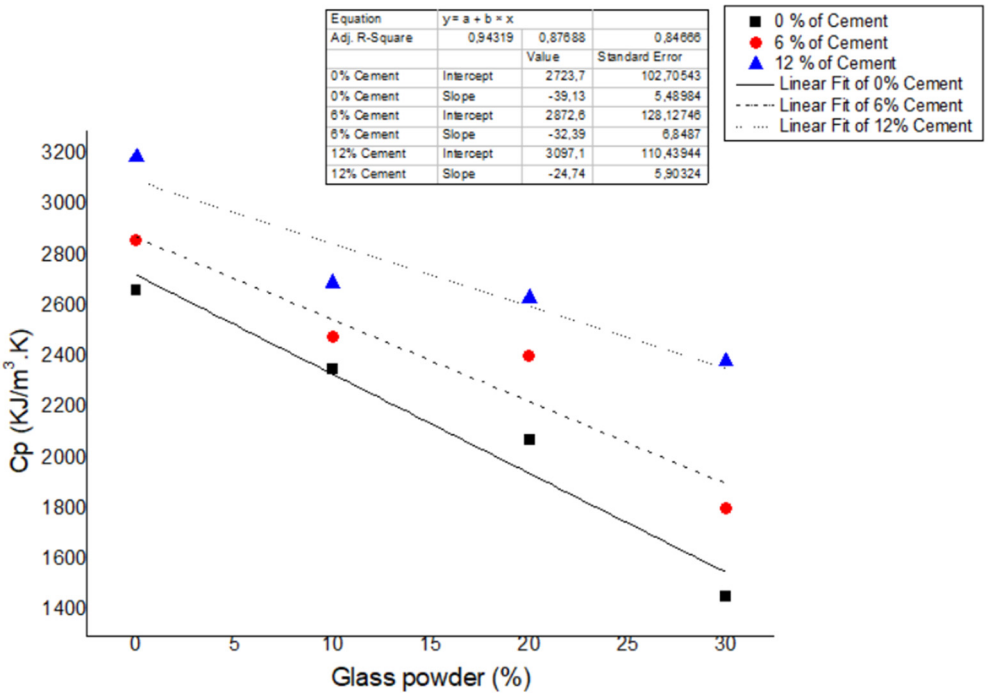


Figure 10. Variation of the measured mortars specific heat capacity in the dry state as a function of the glass powder content.

The specific heat capacity depends mainly on the volume fractions and specific heats of the different components of a composite material [27]. The decrease in the specific heat capacity of the samples with the percentage of the glass powder can be explained by the different volume fractions.

The increase in the percentage of glass powder led to a decrease in the percentage of red earth. However, Nicolas et al. confirmed the decrease in the specific heat capacity of this composite material due to the low value of the specific heat of the glass (913 J/kg·K) and of the air (1005 J/kg·K) present in the pores [27].

Figure 10 also shows an increase in the specific heat capacity of the samples with the addition of 6% and 12% cement. This increase was due to cement particles occupying the pores, which led to a decrease in the number of empty pores. Nevertheless, the specific heat of cement is higher than that of air, which contributed to the increase in the specific heat of the ternary composite material.

3.2.3. Effect of Glass Powder Content on Thermal Diffusivity and Thermal Effusivity

Thermal diffusivity is the quotient of thermal conductivity over specific heat capacity. Figure 11 shows the results deduced from the following relationship:

$$d = \lambda/Cp, \quad (1)$$

where d is the thermal diffusivity, λ is the thermal conductivity, and Cp is the volumetric specific heat.

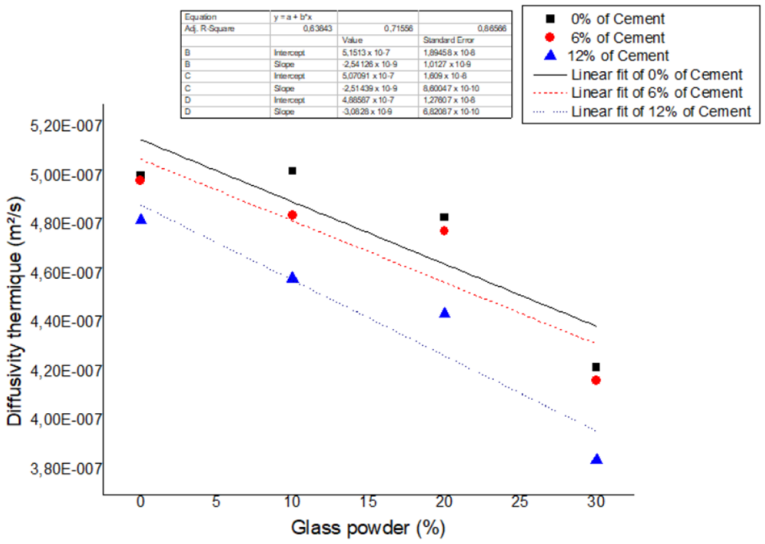


Figure 11. Variation of the thermal diffusivity of the measured mortars in the dry state as a function of the glass powder content.

The thermal diffusivity of the glass powder-substituted earth blocks decreased by an average of 15.66%, 16.37%, and 20.30% with the addition of 0%, 6%, and 12% cement, respectively. The decrease in this thermophysical parameter depended mainly on the decrease in the thermal conductivity and the specific heat of these same composite materials.

The thermal effusivity is presented in the following equation:

$$e = \sqrt{\lambda} \times Cp, \quad (2)$$

where e is the thermal effusivity, λ is the thermal conductivity, and Cp is the volumetric specific heat.

The thermal effusivity values shown in Figure 12 were calculated according to Equation (2). The thermal effusivity of the same specimens substituted with glass powder decreased, on average, by 49.88%, 42.30%, and 33.26% with the addition of 0%, 6%, and 12% cement, respectively.

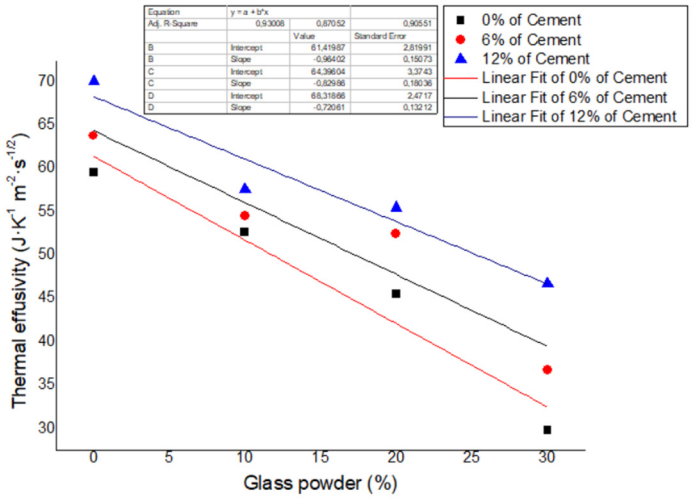


Figure 12. Variation of the thermal effusivity of the measured mortars in the dry state as a function of the glass powder content.

4. Conclusions

The main objective of this study was the use of local materials (red earth) and waste glass powder to establish an economic material with interesting thermophysical behavior. The durability of these new ecological materials according to their use remains acceptable.

In view of its thermophysical behavior, we can draw the below conclusions.

According to EDX results and DRX analysis, the glass powder was characterized by a high content of glass formers and low content of glass modifiers, confirming that the choice of soda-lime glass promoted pozzolanic reactions. The red earth was characterized by its high silica, alumina, and iron oxide content. The DRX analysis confirmed that the main constituents of this material are quartz and muscovite.

Scanning electron microscope analysis also allowed us to confirm the thermophysical behavior of this ternary composite material. The samples without cement were more unfavorable in terms of pore volume. The strong bonds in the cement–red earth matrix confirmed that the material was more compact and, therefore, less porous.

The addition of the stabilizing cement in the red earth substituted by glass powder favored the increase in the thermophysical properties at ambient temperature. This cement stabilization was intended to promote the compactness of the material for its use.

The thermal conductivity of cement-stabilized earth blocks substituted with glass powder decreased with bulk density. The incorporation of 30% glass powder decreased the thermal conductivity by 53.97% (from 1.334 W/m·K to 0.614 W/m·K).

The thermal interest of this material lies in its incorporation of glass powder.

For an equivalent quantity of cement (12%), it is important to compare the effect of the glass powder on the thermophysical behavior of the red earth bricks.

There are still other interesting ways to stabilize the red earth using more ecological and environmental materials instead of cement.

The use of these bricks of stabilized red earth in cement and substituted by glass powder will be the object of future specific research in view of its high economic and environmental significance.

This study did not take into account the control of ASR. This will be the subject of future research. Nevertheless, the choice of the type of glass containing a high percentage of glass formers compared to glass modifiers was taken into account, as well as a minimization of the percentage of glass powder substitution to 30%.

The composite material characterization in this study did not take into account mechanical behavior. This study could be the subject of further research. The composite material could be used as a nonstructural element in the building sector, for elements supporting only their own weight, such as separation walls. However, this field of application should be confirmed by a study that examines the mechanical parameters such as compressive strength, traction, Young's modulus, and resistance to water.

Author Contributions: Conceptualization, O.N. and A.S.; methodology, A.H.A.; software, N.B.; validation, A.S. and A.H.A.; formal analysis, H.S.E.I.; resources, O.N.; data curation, H.S.E.I.; writing—original draft preparation, O.N.; writing—review and editing, A.S.; visualization, A.S.; supervision, A.S. All authors have read and agreed to the published version of the manuscript.

Funding: This research received no external funding.

Institutional Review Board Statement: Not applicable.

Informed Consent Statement: Not applicable.

Data Availability Statement: Not applicable.

Acknowledgments: The authors would like to thank the UATRS-CNRST for the scanning electron microscopy performed for the tests.

Conflicts of Interest: The authors declare no conflict of interest.

References

1. Nguyen, H.P.; Mueller, A.; Nguyen, V.T.; Nguyen, C.T. Development and characterization of lightweight aggregate recycled from construction and demolition waste mixed with other industrial by-products. *Constr. Build. Mater.* **2021**, *313*, 125472. [CrossRef]
2. Kongkajun, N.; Laitila, E.A.; Ineure, P.; Prakaypan, W.; Cherdhirunkorn, B.; Chakartnarodom, P. Soil-cement bricks produced from local clay brick waste and soft sludge from fiber cement production. *Case Stud. Constr. Mater.* **2020**, *13*, e00448. [CrossRef]
3. Colombo, B.; Gaiardelli, P.; Dotti, S.; Caretto, F.; Coletta, G. Recycling of Waste Fiber-Reinforced Plastic Composites: A Patent-Based Analysis. *Recycling* **2021**, *6*, 72. [CrossRef]
4. Antonio, L.; Fern, E.; Salas-morera, L.; Suescum-morales, D. Effect of the Composition of Mixed Recycled Aggregates on Physical—Mechanical Properties. *Crystals* **2021**, *11*, 1518. [CrossRef]
5. Rida, L.; Bazzar, K.; Alaoui, A.H. High-Volume Fly Ash Mortar Solution for Sustainable Development. *Adv. Intell. Syst. Comput.* **2020**, *1104 AISC*, 386–395. [CrossRef]
6. Boussaid, S.; El Bakkouri, A.; Ezbakhe, H.; Ajzoul, T.; El Bouardi, A. Comportement thermique de la terre stabilisée au ciment. *Rev. Française Génie Civ.* **2001**, *5*, 505–516. [CrossRef]
7. Hany, E.; Fouad, N.; Abdel-wahab, M.; Sadek, E. Investigating the mechanical and thermal properties of compressed earth bricks made by eco-friendly stabilization materials as partial or full replacement of cement. *Constr. Build. Mater.* **2021**, *281*, 122535. [CrossRef]
8. Saidi, M.; Cherif, A.S.; Zeghmati, B.; Sediki, E. Stabilization effects on the thermal conductivity and sorption behavior of earth bricks. *Constr. Build. Mater.* **2018**, *167*, 566–577. [CrossRef]
9. Mansour, M.B.; Jelidi, A.; Cherif, A.S.; Jabrallah, S. Optimizing thermal and mechanical performance of compressed earth blocks (CEB). *Constr. Build. Mater.* **2016**, *104*, 44–51. [CrossRef]
10. Nasry, O.; Samaouali, A.; Belarouf, S.; Moufakkir, A.; Sghiouri El Idrissi, H.; Soulami, H.; El Rhaffari, Y.; Hraita, M.; Fertahi, S.E.D.; Hafidi-Alaoui, A. Thermophysical properties of cement mortar containing waste glass powder. *Crystals* **2021**, *11*, 488. [CrossRef]
11. Du, H.; Tan, K.H. Properties of high volume glass powder concrete. *Cem. Concr. Compos.* **2017**, *75*, 22–29. [CrossRef]
12. Mohammadyan-Yasouj, S.E.; Ghaderi, A. Experimental investigation of waste glass powder, basalt fibre, and carbon nanotube on the mechanical properties of concrete. *Constr. Build. Mater.* **2020**, *252*, 119115. [CrossRef]
13. Du, Y.; Yang, W.; Ge, Y.; Wang, S.; Liu, P. Thermal conductivity of cement paste containing waste glass powder, metakaolin and limestone filler as supplementary cementitious material. *J. Clean. Prod.* **2021**, *287*, 125018. [CrossRef]
14. Cengizler, H.; Koç, M.; Şan, O. Production of ceramic glass foam of low thermal conductivity by a simple method entirely from fly ash. *Ceram. Int.* **2021**, *47*, 28460–28470. [CrossRef]
15. Østergaard, M.B.; Cai, B.; Petersen, R.R.; König, J.; Lee, P.D.; Yue, Y. Impact of pore structure on the thermal conductivity of glass foams. *Mater. Lett.* **2019**, *250*, 72–74. [CrossRef]
16. Bignozzi, M.C.; Saccani, A.; Barbieri, L.; Lancellotti, I. Glass waste as supplementary cementing materials: The effects of glass chemical composition. *Cem. Concr. Compos.* **2015**, *55*, 45–52. [CrossRef]
17. Hou, X.; Struble, L.J.; Kirkpatrick, R.J. Formation of ASR gel and the roles of C-S-H and portlandite. *Cem. Concr. Res.* **2004**, *34*, 1683–1696. [CrossRef]
18. Zhang, L.; Gustavsen, A.; Jelle, B.P.; Yang, L.; Gao, T.; Wang, Y. Thermal conductivity of cement stabilized earth blocks. *Constr. Build. Mater.* **2017**, *151*, 504–511. [CrossRef]
19. Ouedraogo, K.A.J.; Aubert, J.E.; Tribout, C.; Escadeillas, G. Is stabilization of earth bricks using low cement or lime contents relevant? *Constr. Build. Mater.* **2020**, *236*, 117578. [CrossRef]
20. Boffoue, M.O.; Kouadio, K.C.; Kouakou, C.H. Influence de la teneur en ciment sur les propriétés thermomécaniques des blocs d'argile comprimée et stabilisée. *Afr. Sci. Rev. Int. Des Sci. Technol.* **2015**, *11*, 35–43. [CrossRef]
21. Shubbar, A.A.; Sadique, M.; Kot, P.; Atherton, W. Future of clay-based construction materials—A review. *Constr. Build. Mater.* **2019**, *210*, 172–187. [CrossRef]
22. Meukam, P. Caractérisation de Matériaux Locaux en Vue de L'isolation Thermique de Batiments. Ph.D. Thesis, Université de Yaoundé I, Yaoundé, Cameroon, December 2004.
23. Ez-Zaki, H.; El Gharbi, B.; Diouri, A. Development of eco-friendly mortars incorporating glass and shell powders. *Constr. Build. Mater.* **2018**, *159*, 198–204. [CrossRef]
24. Jiang, Y.; Ling, T.C.; Mo, K.H.; Shi, C. A critical review of waste glass powder—Multiple roles of utilization in cement-based materials and construction products. *J. Environ. Manag.* **2019**, *242*, 440–449. [CrossRef] [PubMed]
25. Tang, A.M.; Cui, Y.J.; Le, T.T. A study on the thermal conductivity of compacted bentonites. *Appl. Clay Sci.* **2008**, *41*, 181–189. [CrossRef]
26. Tiskatine, R.; Bougdour, N.; Oaddi, R.; Gourdo, L.; Rahib, Y.; Bouzit, S.; Bazgaou, A.; Bouirden, L.; Ihlal, A.; Aharoune, A. Thermo-physical analysis of low-cost ecological composites for building construction. *J. Build. Eng.* **2018**, *20*, 762–775. [CrossRef]
27. Nguyen, L.H. Béton de Structure à Propriétés D'isolation Thermique Améliorées: Approche Expérimentale et Modélisation Numérique. Ph.D. Thesis, University of Cergy Pontoise, Cergy, France, October 2013.